Preparation and characterization of phosphine oxide based polyurethane/silica nanocomposite via non-isocyanate route

Zuhal Hoşgör[a,b], Nılhan Kayaman-Apohan[a,*], Sevim Karataş[a], Yusuf Menceloğlu[c], Atilla Güngör[a]

[a] Department of Chemistry, Faculty of Art and Science, Marmara University, Goztepe 34722, Istanbul, Turkey
[b] Department of Chemistry, Faculty of Art and Science, Trakya University, Edirne, Turkey
[c] Faculty of Engineering and Natural Sciences, Sabancı University, Tuzla 34956, Istanbul, Turkey

ARTICLE INFO

Article history:
Received 3 December 2009
Received in revised form 16 July 2010
Accepted 26 July 2010

Keywords:
Nanocomposites
Polyurethanes
Structure–property relations
Nanoparticles

ABSTRACT

A novel carbonate-modified bis(4-glycidyloxy phenyl) phenyl phosphine oxide (CBGPPO) was synthesized to prepare phosphine oxide based polyurethane/silica nanocomposites. Spherical silica particles were prepared according to Stöber method and modified with cyclic carbonate functional silane coupling agent (CPS) to improve the compatibility of silica particles and organic phase. The cyclic carbonate-modified epoxy resins and silica particles were used to prepare hybrid coatings using hexamethylene diamine as a curing agent. The cupping, impact and gloss measurements were performed on aluminum panels, and the tensile test, gel content, thermal and morphological analyses were conducted on the free films. No damage was observed in the impact strength of the coatings. Incorporation of silica and CBGPPO into formulations increased modulus and hardness of the coating making the material more brittle. It was also observed that, the thermal stability of hybrid coatings enhanced with the addition of silica and CBGPPO.

1. Introduction

Silica precursor particles occupy a prominent position in scientific research, because of their easy preparation and their wide uses in various industrial applications, such as stabilizers, coatings, emulsifiers, strengtheners, binders. The quality of some of these products is highly dependent on the size and size distribution of these particles [1,2]. Stöber et al. [3], in 1968, reported a innovative method for the synthesis of spherical and monodisperse silica nanoparticles that range in size from 50 nm to 1 μm, based on a hydrolysis and condensation reactions of silicon alkoxides in the presence of ammonia as a catalyst. Last 10 years, the research activities have been immensely focused on the synthesis and characterization of polymeric nanocomposites because of their excellent performances compared to conventional composite materials [4]. The early works on nanocomposite materials demonstrated that the enhancement of mechanical and thermomechanical properties is definitely higher in the case of nanosized particles with respect to micron-sized dispersed [5]. As the nano-scale morphology plays an important role in achieving desired macroscopic properties, to obtain a better compatibility between the particles and the host polymeric material is necessary. The surface modification of the inorganic nanoparticles using acrylic/vinylic or epoxy functional trialkoxysilanes is recommended. The formation of chemical bonds between the inorganic and organic components is expected to be of great importance to guarantee a durable chemical junction between the two incompatible phases [6].

Applications of polyurethane (PU) materials have significantly increased in comparison with some other thermosetting polymer materials. Conventional polyurethanes have good mechanical properties but they are porous and possess poor hydrolytic stability and insufficient permeability. The involvement of toxic components, such as isocyanates, in their fabrication process makes the production extremely toxic and dangerous. In this sense, a pioneering method, which depends on the reaction between cyclocarbonate oligomers and primary amine oligomers, has been developed for environmental friendly PU manufacturing [7]. Cyclocarbonates that can be synthesized from corresponding epoxy precursors are attracting research interest due to their potential use in the preparation of green, porous free and moisture insensitive polyurethanes. In non-isocyanate route an intra-molecular hydrogen bond through the hydroxy group at the β-carbon atom of the polyurethane chain is formed. The blockage of carbonyl oxygen considerably lowers the susceptibility of the whole urethane group to hydrolysis. Moreover, materials containing intra-molecular hydrogen bonds display chemical resistance 1.5–2 times more as compared to materials of the similar chemical structure without

* Corresponding author. Tel.: +90 216 3479641; fax: +90 216 3478783.
E-mail address: napohan@marmara.edu.tr (N. Kayaman-Apohan).

such bonds. Production of non-volatile by-products makes this reaction environmental friendly [8–13].

A feasible approach for improving flame retardation of polyurethanes involves the synthesis of phosphorus containing polyurethanes. Since traditional halogen-based flame-retardants have disadvantages such as the potentiality of corroding metal components and toxic corrosive fumes of hydrogen halide during the combustion, halogen-free flame-retardants for polymers have attracted more attention from scientists in recent years. Phosphorus compounds are well established as components of flame-retardant additives. The action of phosphorus containing flame-retardant can occur predominantly through a condensed phase mechanism in which combustion of the outer layers of the polymeric material containing the flame-retardant leads to intumescent carbonaceous char. This acts as a physical and thermal barrier to further combustion, by impeding heat transfer to the underlying layers of polymer and therefore, impeding the release of further flammable volatiles. Other interesting features of environmentally friendly phosphorus polymers are good adhesion to substrates, metal ion binding characteristics and increased polarity. Among these, the phosphine oxide groups have the advantage of containing the hydrolytically stable P–C bond (compared to P–O–C) and the oxidatively stable P═O bond (compared to phosphine). Polymers containing phosphine oxide moieties typically display good flame-retardant property, high thermal oxidative stability, enhanced solubility, and improved miscibility and adhesion [14–22].

The main objective of this work is to develop environmentally friendly and flame-retardant polyurethane–silica nanocomposite coatings. Therefore, two different series of nanocomposites were prepared to investigate the effects of silica nanoparticles and phosphine oxide based cyclocarbonate oligomer on the coating properties. In the first series, the amount of (4-((3-(trimethoxysilyl)propoxy)methyl)-1,3-dioxolan-2-one CPS) modified silica particles were changed gradually in the nanocomposite composition. In the second series, carbonate-modified commercial epoxy oligomers were steadily replaced with carbonate-modified bis(4-glycidyloxy phenyl) phenyl phosphine oxide (CBGPPO) resin in the nanocomposite formulations bearing 4 wt% CPS modified silica content. Nanocomposite coatings were prepared by curing these formulations with diamine thermally and their characterization was performed by analyses of various properties such as impact, cupping, gel content and stress–strain tests. Thermal behaviors and morphologic properties of the coatings were also investigated.

2. Experimental

2.1. Materials

Dichlorophenylphosphine oxide, p-bromo fluoro benzene, magnesium, epichlorohydrin and hexamethylene diamine were purchased from Fluka. Cycloaliphatic diepoxy (Cyracure UV-6107, epoxy group content: 131–140 mmol/kg) was kindly supplied by Dow Chemical. (Polypropyleneglycol) diglycidyl ether (PPG-DGE) with a molecular weight of 640 g/mol, (3-glycidyloxypropyl) trimethoxysilane (GPTMS) and tetrabutylammonium bromide (TBAB) were purchased from Sigma–Aldrich. Tetramethylorthosilicate (TMOS), hexamethylene diamine (HMDA) and triphenyl phosphine were purchased from Merck AG. BYK 333 as wetting agent was obtained from BYK Chemie. Common solvents such as tetrahydrofurane, methanol, acetone and all materials were used as received. All other chemicals were of analytical grade and were purchased from Merck AG. Anode oxidized aluminum panels (75 mm × 150 mm × 0.82 mm) were used as substrates in all coating applications.

2.2. Characterization

The chemical structures of synthesized resins were identified by FT-IR (Shimadzu 8300 FT-IR). The solid state cross-polarization (CP)/magic-angle spinning (MAS) ^{29}Si NMR spectrum was recorded using a Bruker Avance Superconducting FT NMR Spectrometer operated at 300 MHz. 13C spectrum was recorded using Mercury-VX 400 BB model NMR operated at 400 MHz.

SEM (scanning electron microscope) imaging was performed on a JEOL-JSM-5919LV. SEM micrographs were taken by dropping silica nanoparticles dispersed in methanol on carbon platform and drying under vacuum before gold sputtering. Measurement of the mean particle diameter of the carbonate functional silica particles was conducted with the use of a dynamic light scattering particle size analyzer that had a measuring range of 0.6 nm to 6 mm (Zetasizer Nano ZS, Malvern Instruments Ltd., Worcestershire, UK). Refractive indices of 1.46 for silica and 1.328 for methanol were used to calculate the particle size. The temperature was 20 °C. The final particle diameter was calculated from the average of at least three measurements.

For TEM investigation, the silica particles dispersed in poly(ethyleneglycol diacrylate) was diluted with pure acetone and sprayed on Cu grids. Wet formulation is cured with UV irradiation. TEM-work was performed using a JEOL 1011B operated at 80 kV in order to enhance the contrast between the polymer matrices and the silica particles.

Thermogravimetric analyses (TGA) were conducted with Netzsch STA 409 CD in air atmosphere using a heating rate of 10 °C/min over the temperature range of ca. ambient to 900 °C. Differential scanning calorimetry (DSC) analyses of the films were obtained using Perkin Elmer DSC Pyris Diamond model device. Samples were run under a nitrogen atmosphere from −80 to +80 °C with a heating rate of 10 °C/min.

The coating properties were measured in accordance with the corresponding standard test methods as indicated; gloss (ASTM D-523-80), impact (ASTM D-2794-82) and cupping test (DIN 53156).

The gel contents of the hybrid films were determined by Soxhlet extraction method for 4 h employing acetone.

Mechanical properties of the free films were determined by standard tensile stress–strain tests in order to measure the modulus (E), ultimate tensile strength (σ) and elongation at break (ε). Stress–strain measurements were carried out at room temperature using a universal test machine (Zwick Rolle, 500N) with a crosshead speed of 10 mm/min. The measurements represent the average of at least five runs.

2.3. Synthesis of the materials

2.3.1. Synthesis of silica nanoparticles

Silica particles were prepared by hydrolysis and condensation of tetramethylorthosilicate (TMOS) in methanol (MeOH) with ammonia (NH_3) as the base catalyst causing the formation of spherical particles according to Stöber method [3]. 10 mmol TMOS and half volume of the methanol (5 ml) were charged into three-necked flask, equipped with a mechanical stirrer, a dropping funnel and a condenser, heated to 50 °C. Then the solution of 1 mmol ammonia, 40 mmol water and residual half of the methanol (5 ml) was slowly dropped into the flask and stirred at 50 °C for 19 h to obtain silica particles. The silica particles were washed with dichloromethane several times to remove ammonia and dried in vacuum at 80 °C [23,24].

2.3.2. Synthesis of carbonate functional silica particles (Si-CPS)

In order to prepare non-isocyanate polyurethane/silica nanocomposites, surface of the silica particles required carbonate modification. For that purpose, initially, carbonate modification

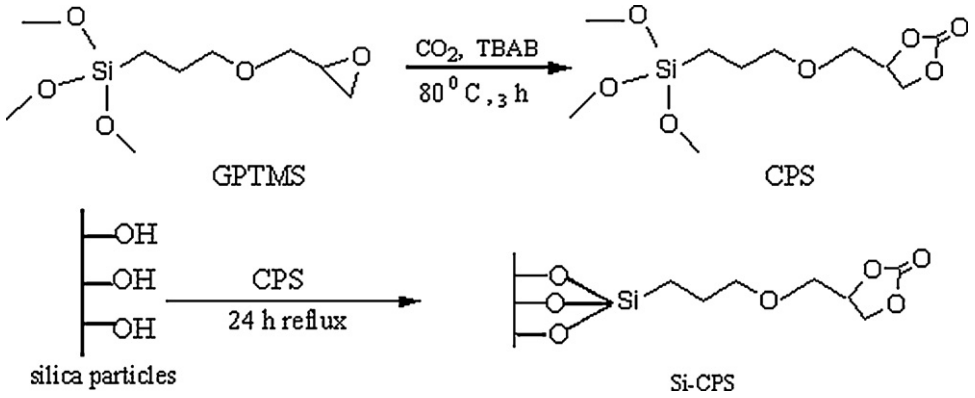

Scheme 1. Synthesis reaction of carbonate-modified silica (Si-CPS).

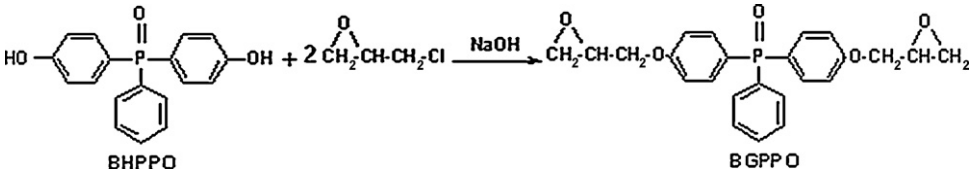

Scheme 2. Synthesis reaction of BGPPO.

of silane coupling agent (3-glycidyloxypropyl) trimethoxysilane (GPTMS) was performed in supercritical conditions (2000 psi) at 100 °C in 3 h using 5 wt% of tetrabutylammonium bromide (TBAB) catalyst which was removed by washing with dichloromethane and water [25].13.3 ml of carbonate functional silane coupling agent 4-(3-(trimethoxysilyl)propoxyl)methyl-1,3-dioxolan-2-one (CPS) and 240 μl of triethylamine were added into 10 g of silica particles stirred in 300 ml of freshly distilled toluene. The mixture was stirred for further 24 h at 65 °C. Then non-bonded CPS was removed by centrifuge and extraction with toluene, dichloromethane and acetone respectively [26,27]. The functionalized silica particles were finally dried in vacuum at 50 °C. A representation of this reaction is shown in Scheme 1.

2.3.3. Synthesis of bis(4-glycidyloxy phenyl) phenyl phosphine oxide (BGPPO)

The synthesis of bis(4-hydroxy phenyl) phenyl phosphine oxide (BHPPO), which was the precursor of (4-glycidyloxy phenyl) phenyl phosphine oxide (BGPPO), was performed according to literature [12–14]. Briefly, bis(4-fluoro phenyl) phenyl phosphine oxide (BFPPO) was synthesized via Grignard reaction and then BHPPO was prepared by hydrolyzing BFPPO using potassium hydroxide. BHPPO (20 g, 0.064 mol), epichlorohydrin (55.2 ml, 0.698 mol) and isopropyl alcohol (10 ml) were charged into 250 ml three-neck round bottom flask equipped with reflux condenser, mechanical stirrer, a dropping funnel and a nitrogen inlet. 19.4 g of 30 wt% aqueous NaOH was dropped into the flask over a period of half an hour and further reacted at the reflux temperature for 2 h. The crude product washed with hot water and toluene [18,19]. The organic phase was distilled to remove the toluene and the yellow colored viscous epoxy resin (BGPPO) (epoxide equivalent weight, EEW = 294.5) was obtained in a yield about 75%. A representation of this reaction is shown in Scheme 2.

2.3.4. Carbonate modification of epoxy resins

In this stage, in addition to bis(4-glycidyloxy phenyl) phenyl phosphine oxide (BGPPO), two different commercial epoxy resins were also used; (polypropyleneglycol) diglycidyl ether (PPG-DGE)

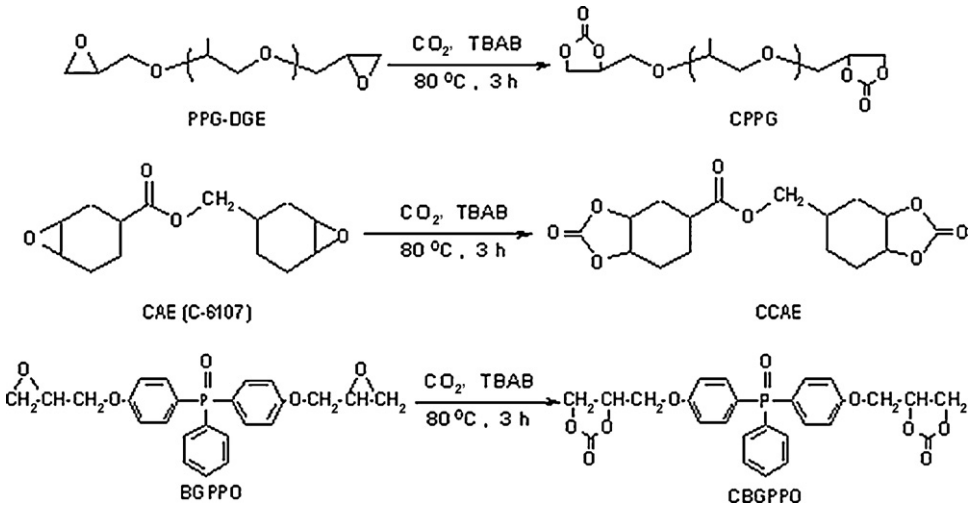

Scheme 3. Synthesis reaction of carbonate modification of epoxy resins.

Table 1
Polyurethane–silica nanocomposite coating formulations.

	Sample	% Silica	Si-CPS (g)	EtOH[a] (g)	CCAE (g)	CPPG (g)	CBGPPO (g)	HMDA (g)	PPh_3 (g)
1	CCAE-PPG-0	0	–	4	5	5	–	3.005	0.075
2	CCAE-PPG-1	1	0.05	4	5	5	–	3.015	0.075
3	CCAE-PPG-1.5	1.5	0.1	4	5	5	–	3.025	0.075
4	CCAE-PPG-2	2	0.2	4	5	5	–	3.035	0.075
5	CCAE-PPG-4	4	0.4	4	5	5	–	3.045	0.075
6	CCAE-PPG-6	6	0.6	4	5	5	–	3.055	0.075
7	CCAE-PPG-CBGPPO-10-4	4	0.4	4	4.5	4.5	1	2.98	0.075
8	CCAE-PPG-CBGPPO-20-4	4	0.4	4	4	4	2	2.95	0.075
9	CCAE-PPG-CBGPPO-30-4	4	0.4	4	3.5	3.5	3	2.92	0.075
10	CCAE-PPG-CBGPPO-20-0	0	0	4	4	4	2	2.95	0.075

[a] BYK/ethanol solution (2 wt%).

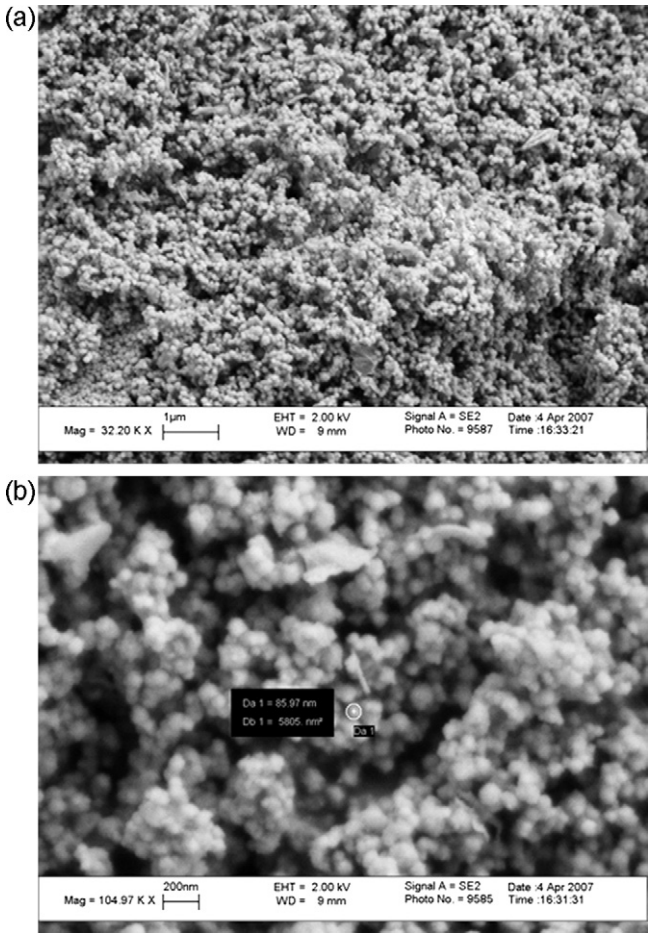

Fig. 1. SEM images of silica particles (a) ×32.20 KX (b) ×104.97 KX.

and Cyracure UV-6107 (cyclic aliphatic epoxy resin). Modification of all epoxy resins was performed in supercritical conditions (1500 psi CO_2) at 80 °C in 3 h using tetrabutylammonium bromide (TBAB) as a catalyst. After extraction with dichloromethane and evaporation, viscous carbonate-modified epoxy resins were obtained in a yield about 90%. A representation of reaction is shown in Scheme 3.

2.3.5. Preparation of phosphine oxide based polyurethane–silica nanocomposite coatings and free films by non-isocyanate route

Firstly, various amounts of modified silica particles were dispersed in ethanol solution that contains BYK as wetting agent and triphenylphosphine (TPP) as a catalyst over a period of 2 h in a sonication bath. After the addition of carbonate-modified epoxy resins, ethanol was removed in vacuum oven at 75 °C. Finally hexamethylene diamine (HMDA) as a curing agent was added to the formulation. The compositions of all coating formulations were given in Table 1. In order to remove air bubbles formed during mixing; formulations heated to 35 °C then kept under gentle vacuum for 10 min without upsetting composition. After removal of air bubbles the prepared formulations were applied on to aluminum panels using a wire gauged bar applicator in order to obtain uniform thickness of 30 μm and left at 100 °C for 24 h to cure. Moreover, hybrid free films were prepared by pouring the liquid formulations on to a Teflon® mold (10 mm × 50 mm × 1 mm) and cured at 100 °C for 24 h.

3. Results and discussion

Silica nanoparticles was synthesized according to Stöber method. Morphologic characterization of particles was carried out by SEM analyses. The morphology of silica particles was shown in Fig. 1a and b. SEM images indicate that silica particles were agglomerated while they were drying. Their particle size was around 100 nm. The morphology of particles was also investigated by TEM. TEM picture shows that although there are lots off small particles less than 50 nm, particles around 100–150 nm sizes can also be detected due to combination of smaller ones (Fig. 2)

Carbonate modification reaction of GPTMS was followed by FT-IR and ^{13}C NMR. The success of reaction was understood by the formation of carbonyl of cyclic carbonate peak that occurred at 1790 cm^{-1} and disappearance of epoxy peak at 909 cm^{-1}, in the FT-IR spectrum (Fig. 3). The appearance of intensive peak at 155 ppm that attributed to carbonyl of cyclic carbonate structure in ^{13}C NMR spectrum of CPS (Fig. 4) was another proof of the successful reaction.

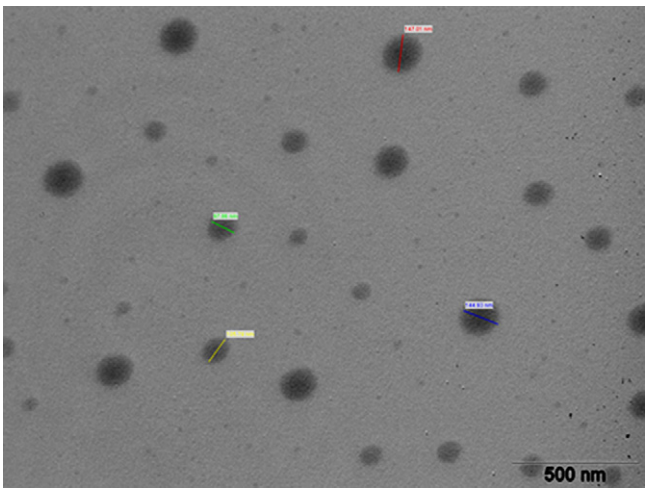

Fig. 2. TEM image of silica particles.

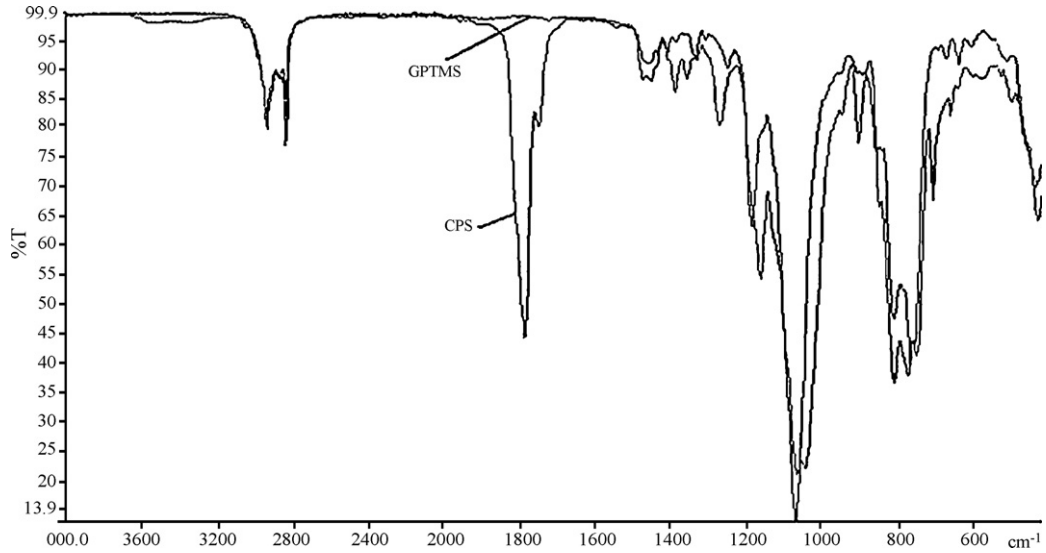

Fig. 3. FT-IR spectra of CPS and GPTMS.

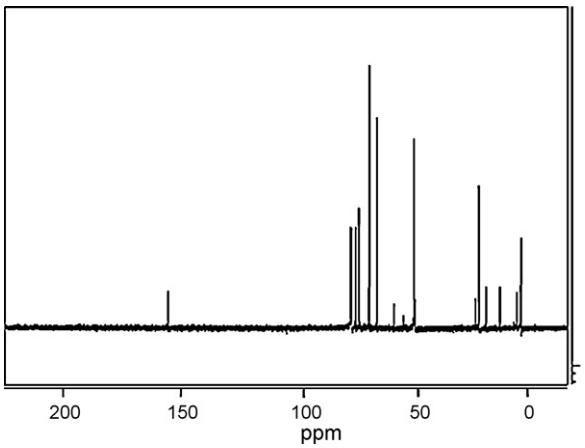

Fig. 4. ^{13}C NMR spectrum of CPS.

Synthesis of silane coupling agent CPS is followed by modification of silica particles. The success of the CPS modification can be verified by FT-IR and solid state CP/MAS ^{29}Si NMR measurements. Fig. 5 shows the FT-IR spectra of silica particles with and without surface modification. The appearance of peaks at 1738 cm^{-1} and 2970 cm^{-1} belonging to CPS in the FT-IR spectra of modified silica particles indicates that carbonate modification of silica particles achieved successfully. In the ^{29}Si NMR spectrum, peaks in the T region are contributed by Si atoms of trialkoxysilane while those in the Q region arise from Si atoms of TMOS. In the other words, T^n represents Si atoms joined to the organic group, bearing (3-*n*) uncondensed SiOH groups and forming n Si–O–Si bonds. Q^n represents a Si atom of TMOS forming *n* Si–O–Si bonds and bearing (4-*n*) OH groups [28–31]. In ^{29}Si NMR spectrum of modified silica particles (Fig. 6) showed both Q peaks around 122 ppm and T peaks around 70–75 ppm. Since one can say that the covalent bond formed between silylating agent and silanol groups on the silica surface.

Measurement of the mean particle diameter of the carbonate functional silica particles was conducted with the use of a dynamic light scattering particle size analyzer Malvern Zetasizer-ZS. The carbonate functional silica particle's size was analyzed by preparing their suspension in deionised water. Particle size measurement indicated that they had an average diameter of 402 nm with a polydispersity index of 0.74 (Fig. 7). The PDI is a measure of dispersion homogeneity and ranges from 0 to 1. Values close to 0 indicate a homogeneous dispersion while those greater than 0.3 indicate high heterogeneity [32]. As can be seen in DLS result the larger particle size could be explained on the basis of surface modification. It is possible that the particles become physically joined as a result of the surface modification process. Although the chemical bonding between silica nanoparticles and matrix is very important for increasing density and cross-linking of the coatings, it could also lead to an undesirable agglomeration of nanoparticles.

The carbonate modification of silica particles was also investigated by TGA analysis. Fig. 8 shows that the TGA curves of modified and non-modified silica nanoparticles. As can be seen from Fig. 8, the mass loss of modified and non-modified silica nanoparticles are 30% and 16%, respectively for the whole temperature range. Calculation results show that the 16% weight loss is related to bound water to silica particles, the 14% of weight loss is related with organic part (modification) and the residual part (70 wt%) is due to the silicon dioxide.

BGPPO was synthesized from BHPPO. The chemical structure of BGPPO was characterized by FT-IR. The characteristic absorption peak at 914.6 cm^{-1} for oxirane ring was observed in the FT-IR spectrum of BGPPO shown in Fig. 9. The appearance of –OH peak around 3300 cm^{-1} results from partial opening of epoxy ring and moisture left within resins after extraction. Carbonate modification of epoxy resins was carried out in supercritical conditions. FT-IR spectroscopy was used to follow the reaction. FT-IR spectrum of CBGPPO was also shown in Fig. 9. The appearance of carbonyl peak belonging the cycle carbonate around 1790 cm^{-1} and disappearance of the epoxy peak around 914 cm^{-1} indicated that all epoxy groups were converted into cyclic carbonate structure.

In this study, two different series of formulations were prepared to investigate both effect of silica and phosphine oxide moiety on the coating properties. In the first series, the amount of silica particles were changed gradually while the amount of CCAE-PPG resin mixture (50:50 wt%) in formulation was kept constant. The results from our previous studies indicated that, there was a successful dispersion of phosphine oxide based resins to compose nanocomposite materials. Hence, CBGPPO resin was used in polyurethane synthesis for both dispersing silica particles in organic polymers and enhancing the flame retardancy of the coatings. In the second series, phosphine oxide based carbonate-modified epoxy resins gradually added to the formulation with 4 wt% silica content,

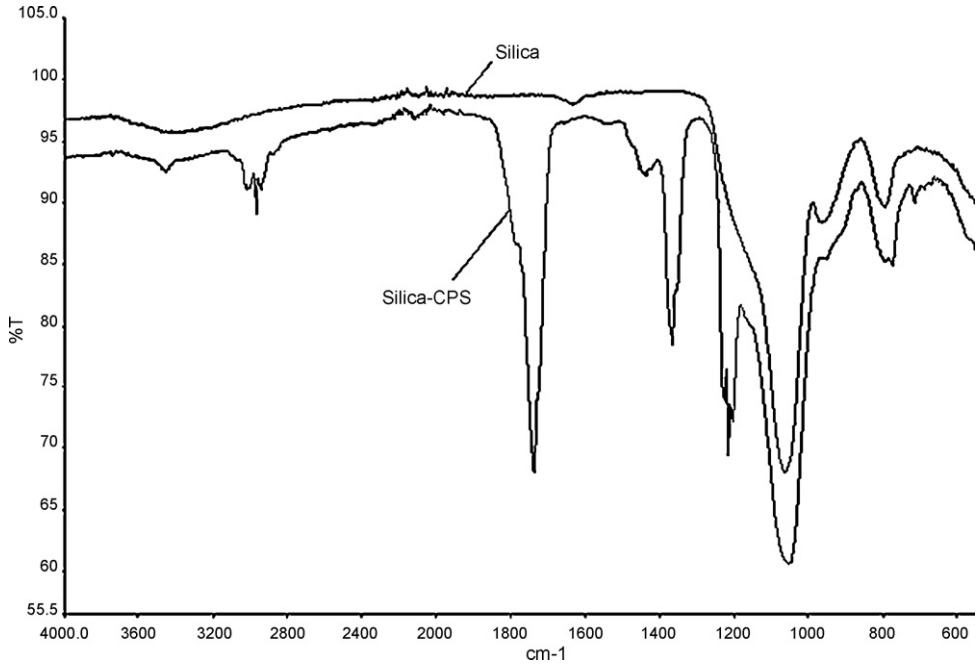

Fig. 5. FT-IR spectra of silica particles without and with surface modification.

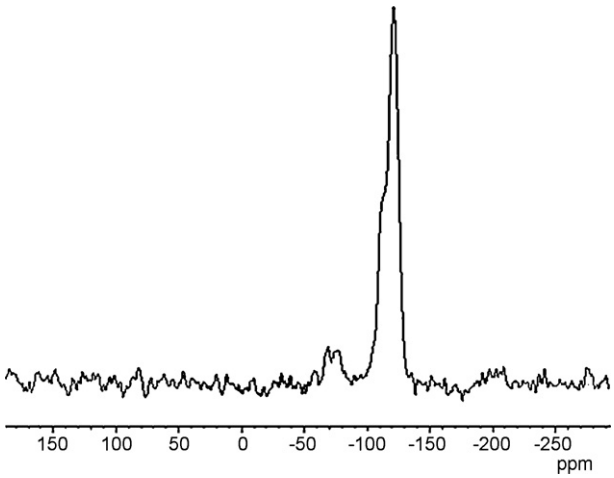

Fig. 6. ^{29}Si NMR spectrum of modified silica particles (Si-CPS).

decreasing the amount of organic matrix (CPPG and CCAE). In all formulations hexamethylene diamine was used to prepare non-isocyanate polyurethane nanocomposites by thermal curing method. Feed compositions that used to prepare aluminum coatings and free films were shown in Table 1.

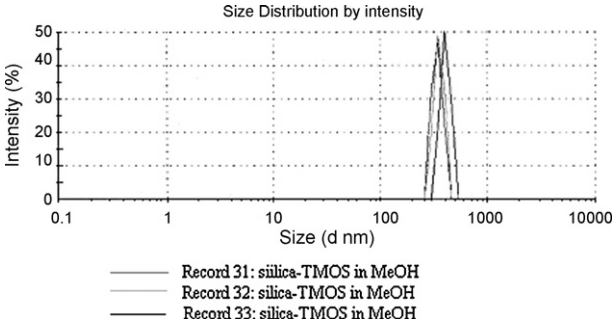

Fig. 7. Particle size of the modified silica particles (Si-CPS).

The coated aluminum panels were subjected to performance tests such as impact and cupping. After impact and cupping tests were applied to aluminum coating no damage was seen.

In order to investigate the surface property of hybrid materials water contact angle measurements were performed. Each contact angle value given in Table 2 represents an average of 8–10 readings. As shown in Table 2, contact angle values increase with incorporation of silica particles and phosphine oxide based resin.

Mechanic properties of polyurethane nanocomposites were investigated with universal tensile test machine. Evaluated stress–strain data of hybrid coatings as Young's modulus, ultimate tensile strength and elongation at break were listed in Table 3 and graphics of them were shown in Fig. 10a and b. As show in the table, in the first series value of modulus and ultimate strength values increased from 3.0 N/mm^2 to 256.2 N/mm^2 and 56.5 kg/cm^2 to 139.3 kg/cm^2 respectively by increasing the silica amount in the coating. While incorporation of silica makes the coating stronger but also makes brittle. Elongation at break is decreasing sharply at 6 wt% silica content because at higher silica concentrations, silica aggregates making the coating more brittle. In the second series, addition of phosphine oxide makes remarkable increase in module values. But at concentration 10 wt% phospine oxide based resin, the ultimate strength reached maximum value since aromatic rigid groups increased the hardness of the coating making the material more brittle.

The thermal properties of the hybrid coatings were characterized by DSC and TGA analyses. The DSC thermograms of the films were shown in Fig. 11. One can say that the incorporation of silica particles does not make significant effect on T_g values but with incorporation of phosphine oxide based resin, T_g values increased from 5 °C to 10 °C. And also all formulations show only a single T_g, which demonstrates the compatibility of three resins.

Fig. 12a and b shows the thermal degradation behaviors of hybrid coatings. TGA measurements were carried out under air atmosphere at heating rate 10 °C/min from room temperature to 900 °C and the test data are summarized in Table 4. All samples showed 5 wt% weight loss between 198 °C and 242 °C implying the release of volatile degradation products such as methanol, the excess amount of HMDA and the moisture of silica parti-

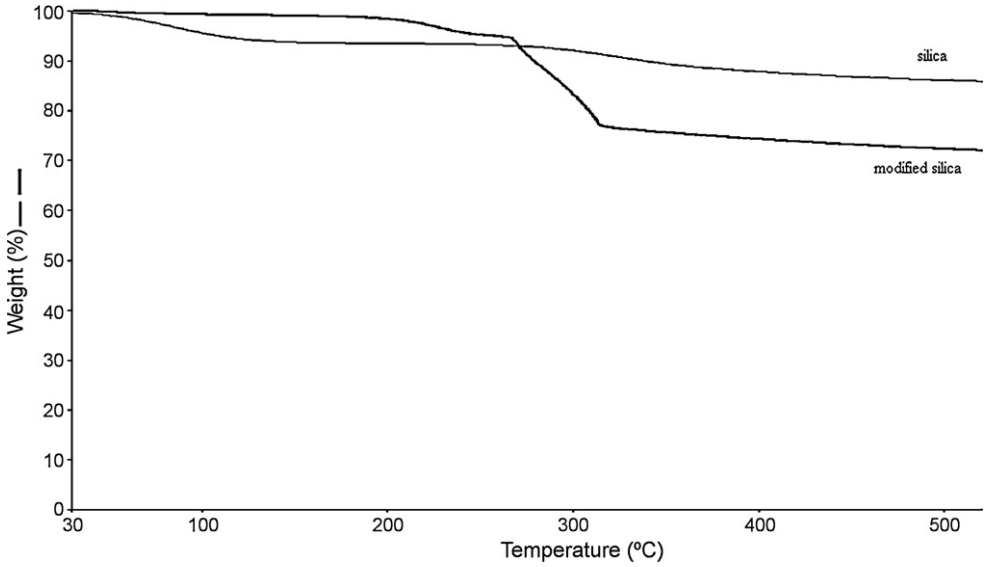

Fig. 8. TGA thermograms of modified and non-modified silica particles.

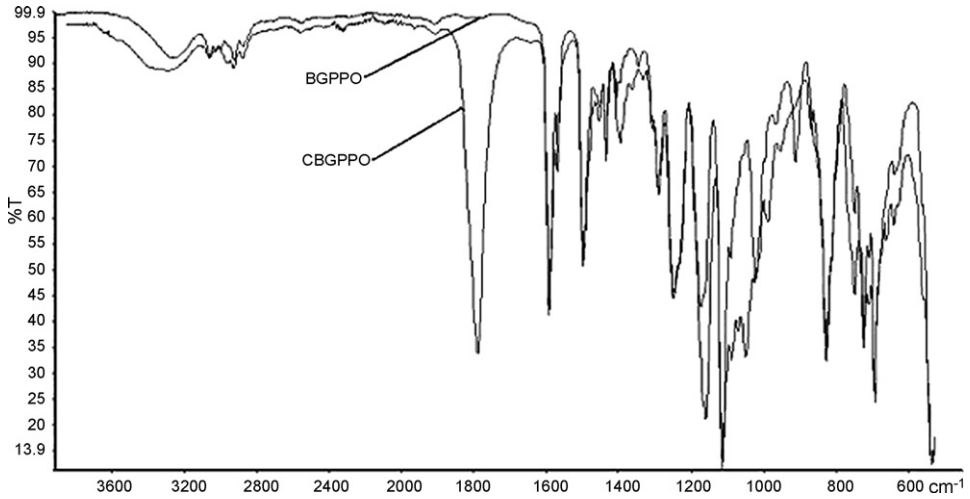

Fig. 9. FT-IR spectra of BGPPO and CBGPPO.

Table 2
Performance tests of coating materials.

Sample	Contact angle	Impact strength[a]	Cupping[a]	Gel content (%)
CCAE-PPG-0	31.0	ND	ND	95
CCAE-PPG-1	34.0	ND	ND	91
CCAE-PPG-1.5	34.4	ND	ND	95
CCAE-PPG-2	35.3	ND	ND	96
CCAE-PPG-4	36.9	ND	ND	95
CCAE-PPG-6	39.3	ND	ND	96
CCAE-PPG-CBGPPFO-10-4	36.5	ND	ND	99
CCAE-PPG-CBGPPFO-20-4	37.0	ND	ND	99
CCAE-PPG-CBGPPFO-30-4	38.5	ND	ND	96
CCAE-PPG-CBGPPFO-20-0	36.9	ND	ND	97

[a] ND = No damage.

cles. One can see that, CCAE-PPG based polyurethane coating were degraded in a three step manner. It is determined that maximum weight loss and second weight loss were realized around 350 °C and 455 °C respectively. After the final weight loss between 564 °C and 612 °C polymer skeleton was completely degraded. It was clearly observed that final weight loss temperature shifted to higher values with increasing silica content, especially with 6% silica content, it was reached maximum value. It was also observed that maximum and second weight loss temperatures decreased with increasing CBGPPO amount. On the other hand there was a significant increase in final weight loss temperatures and char yields. This is a typical flame-retardant characteristic of phosphine oxides. A flame-retardant inhibits combustion by forming a glass-like layer on the coating. The increase in the final weight loss temperature from 582 °C to 657 °C and in the char yield from 1.7 wt% to 4.5 wt% by incorporation of 30 wt% phosphine oxide based carbonate resin

Table 3
Stress–strain analysis of coatings.

Sample	Young modulus (N/mm^2)	Ultimate tensile strength (kg/cm^2)	Elongation (%)
CCAE-PPG-0	3.0	56.5	278.7
CCAE-PPG-1	10.0	92.9	217.0
CCAE-PPG-1.5	16.4	64.0	258.9
CCAE-PPG-2	59.4	89.3	198.0
CCAE-PPG-4	102.3	111.9	185.4
CCAE-PPG-6	256.2	139.3	11.5
CCAE-PPG-CBGPPO-10-4	206.8	132.2	9.6
CCAE-PPG-CBGPPO-20-4	381.7	113.5	5.7
CCAE-PPG-CBGPPO-30-4	660.1	55.9	1.4
CCAE-PPG-CBGPPO-20-0	404.4	58.7	3.4

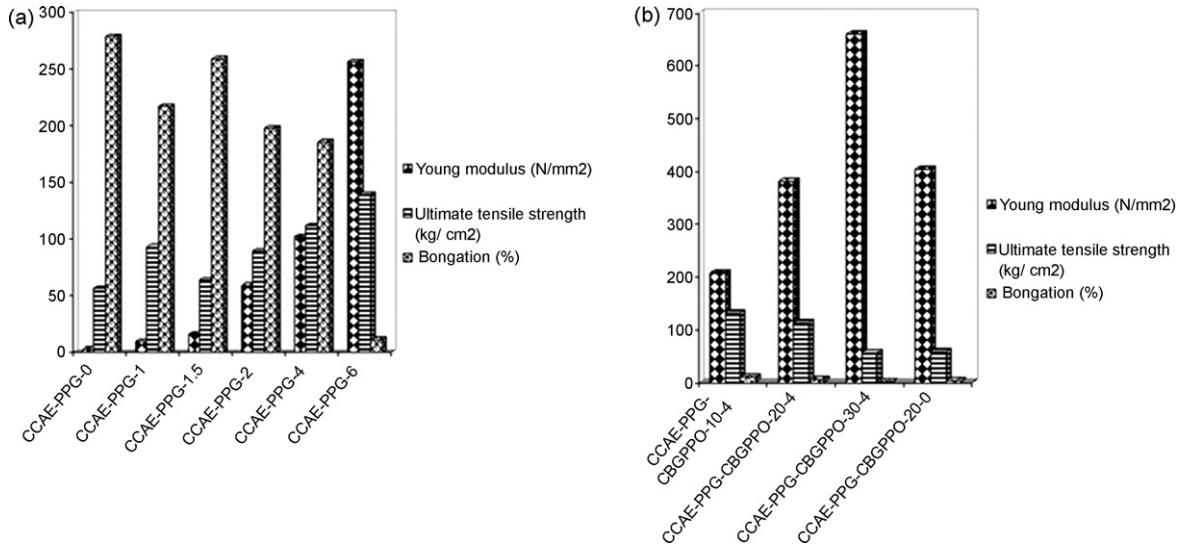

Fig. 10. Stress–strain plots of the hybrid coatings (a) CCAE-PPG based coatings, (b) CCAE-PPG-CBGPPO based coatings.

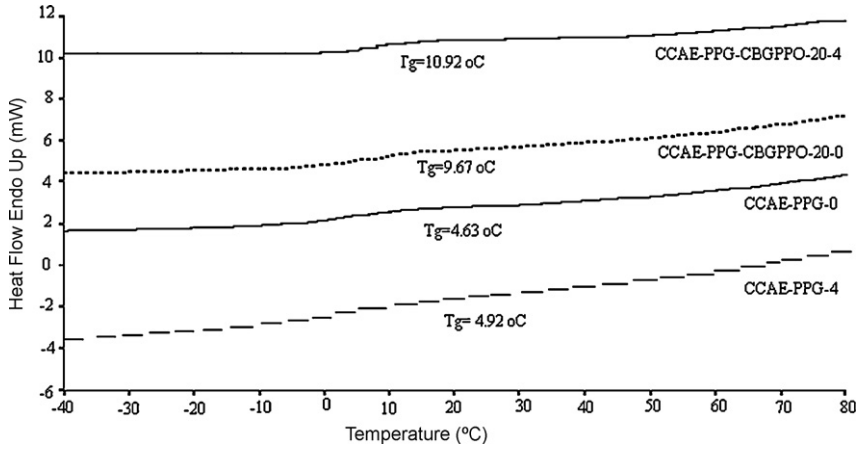

Fig. 11. DSC thermograms of the hybrid coatings.

Table 4
TGA analyses of coating materials.

Sample	5 wt% weight loss (°C)	Maximum weight loss (°C)	Second weight loss (°C)	Third weight loss (°C)	Char yield (%)
CCAE-PPG-0	205	351	455	564	0.60
CCAE-PPG-1	210	353	460	572	0.68
CCAE-PPG-1.5	230	354	470	586	1.23
CCAE-PPG-2	214	353	467	574	1.32
CCAE-PPG-4	198	355	465	582	1.70
CCAE-PPG-6	242	355	465	612	3.49
CCAE-PPG-CBGPPO-10-4	225	335	428	600	2.11
CCAE-PPG-CBGPPO-20-4	233	339	435	633	2.77
CCAE-PPG-CBGPPO-30-4	210	339	441	657	4.44
CCAE-PPG-CBGPPO-20-0	210	357	439	621	1.66

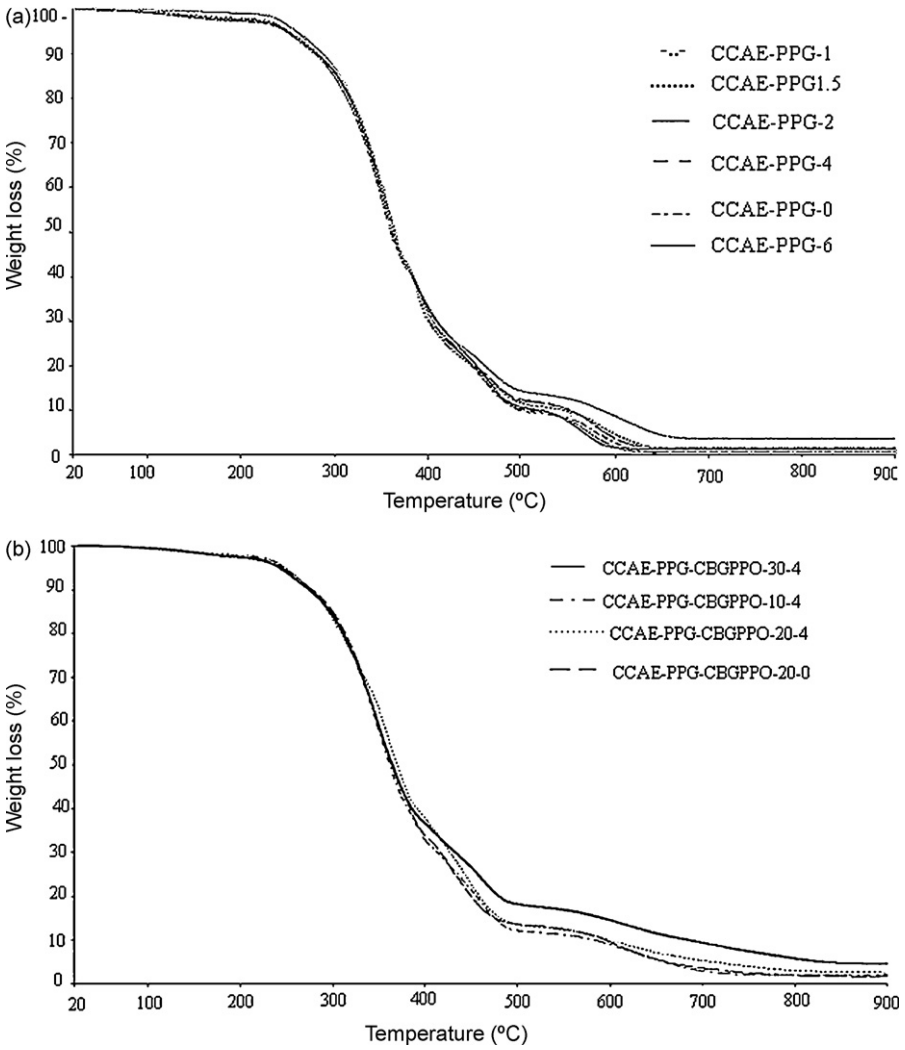

Fig. 12. TGA thermograms of the hybrid coatings (a) CCAE-PPG based coatings, (b) CCAE-PPG-CBGPPO based coatings.

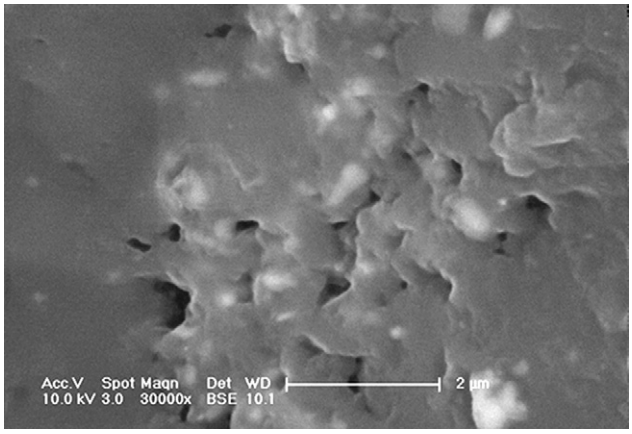

Fig. 13. SEM image of the CCAE-PPG-BGPPFO-20-4 hybrid coating.

indicated that flame retardency and thermal stability of coatings were increased.

The surface morphology of the phosphine oxide containing hybrid coating was investigated by SEM analyses using back scattering method. As shown in Fig. 13, at magnification of 30,000× silica particles can be seen at the surface. Particles were seen as buried because of tree times gold treatment to prevent surface from electron beam. As seen, the average particle size is approximately less than 500 nm and the agglomerated particles distributed through the coating.

4. Conclusions

In this paper, phosphine oxide based polyurethane/silica nanocomposites were synthesized via non-isocyanate route. Spherical silica particles were prepared according to Stöber method from methanol solutions of tetramethylorthosilicate (TMOS) in the presence of ammonia as a catalyst. To improve the compatibility between silica particles and organic part, surface of the silica particles were modified with silane coupling agent, (4-((3-(trimethoxysilyl)propoxy)methyl)-1,3-dioxolan-2-one, CPS), which was synthesized successfully by the carbonate modification reaction of (3-glycidyloxypropyl) trimethoxysilane (GPTMS). The cyclic carbonate resins, prepared from corresponding epoxy precursors, were used to prepare nanocomposite formulations with 0–6 wt% silica content. 0–30 wt% carbonate-modified bis(4-glycidyloxy phenyl) phenyl phosphine oxide (CBGPPO), which was synthesized to add phosphine oxide moiety was incorporated to the formulations with 4 wt% silica content. Finally, formulations were cured thermally with hexamethylene diamine to prepare nanocomposite coatings. The hybrid coating properties such as impact, cupping and tensile strength were investigated. No

damage was observed in the impact strength of the coatings. Incorporation of silica and CBGPPO into formulations increased modulus and hardness of the coating making the material more brittle. It was also observed that, the thermal stability of hybrid coatings enhanced with the addition of silica and CBGPPO. Thermal gravimetric analysis of CBGPPO containing polymeric films gave higher char yield compared with CCAE-PPG only.

Acknowledgements

This work was supported by TUBITAK (The Scientific & Technological Research Council of Turkey) Research Project under grant project number: 106T083.

References

[1] K.S. Rao, K. El-Hami, T. Kodaki, K. Matsushige, K. Makino, J. Colloid Interface Sci. 289 (1995) 125.
[2] D.L. Green, J.S. Lin, Y.F. Lam, M.Z. Hu, D.W. Schaefer, M.T. Harris, J. Colloid Interface Sci. 266 (2003) 346.
[3] W. Stöber, A. Fink, E. Bohn, J. Colloid Interface Sci. 26 (1968) 62.
[4] G. Kickelbick, Prog. Polym. Sci. 28 (2003) 83.
[5] R. Bongiovanni, M. Sangermano, S. Ronchetti, A. Priola, G. Malucelli, Polymer 48 (2007) 7000.
[6] O. Türünç, N. Kayaman-Apohan, M.V. Kahraman, Y. Menceloğlu, A. Gungor, J. Sol–Gel Sci. Technol. 47 (2008) 290.
[7] S. Sarkar, Paintindia 57 (2007) 99.
[8] O.L. Figovsky, L. Shapovalov, Nonisocyanate Polyurethanes for Adhesives and Coatings First International IEEE Conference on Polymers and Adhesives in Electronics, Potsdam, Germany, October 21–24, 2001, p. 257.
[9] O.L. Figovsky, L. Shapovalov, F. Buslov, Surf. Coat. Int. B: Coat. Trans. 88B (2004) 167.
[10] C.D. Diakoumakos, D.L. Kotzev, Macromol. Symp. 216 (2004) 46.
[11] O.L. Figovsky, L. Shapovalov, Macromol. Symp. 187 (2002) 325.
[12] I.V. Stroganov, V.F. Stroganov, Polym. Sci. C 49 (2007) 263.
[13] Y. Du, J.Q. Wang, J.Y. Chen, F. Cai, J.S. Tian, D.L. Kong, L.N. He, Tetrahedron Lett. 47 (2006) 1271.
[14] S. Karataş, Z. Hoşgör, Y. Menceloglu, N. Kayaman-Apohan, A. Gungor, J. Appl. Polym. Sci. 102 (2006) 1906.
[15] C.D. Smith, H. Gurbbs, H.F. Webster, A. Gungor, J.P. Wightman, J.E. McGrath, High Perform. Polym. 3 (1991) 211.
[16] D.J.J. Riley, Ph.D. Thesis, Virginia Polytechnic Institute, 1997.
[17] N. Mann, S.K. Mendon, J.W. Rawlins, S.F. Thames, J. Am. Oil Chem. Soc. 85 (2008) 791.
[18] H. Ren, J. Sun, B. Wu, Q. Zhou, Polym. Degrad. Stab. 92 (2007) 956–961.
[19] M.S. Lakshmi, B.S.R. Reddy, Eur. Polym. J. 38 (2002) 795.
[20] M.V. Kahraman, N. Kayaman-Apohan, N. Arsu, A. Gungor, Prog. Org. Coat. 51 (2004) 213.
[21] M.J. Alcon, G. Ribera, M. Galia, V. Cadiz, Polymer 44 (2003) 7291.
[22] Y.L. Liu, J. Appl. Polym. Sci. 83 (2002) 1697.
[23] Y. Chen, S. Zhou, G. Chen, L. Wu, Prog. Org. Coat. 54 (2005) 120.
[24] Y. Chen, S. Zhou, H. Yang, G. Gu, L. Wu, J. Colloid Interface Sci. 279 (2004) 370.
[25] D.L. Tomasko, H. Li, D. Liu, X.Han, M. Wingert, L.J. Lee, K.W. Koelling, Ind. Eng. Chem. Res. 42 (2003) 6431.
[26] S. Radi, A. Ramdani, Y. Lekchiri, M. Morcellet, G. Crini, L. Janus, M. Bacquet, New J. Chem. 27 (2003) 1224.
[27] A. Ponchel, S. Abramson, J. Quartararo, D. Bormann, Y. Barbaux, E. Monflier, Microporous Mesoporous Mater. 75 (2004) 261.
[28] D.P. Fasce, I.E. Erba, R.J.J. Williams, Polymer 46 (2005) 6649.
[29] X. Zhang, N. Zhao, W. Wei, Y. Sun, Catal. Today 115 (2006) 102.
[30] S.R. Davis, A.R. Brough, A. Atkinson, J. Non-Cryst. Solids 315 (2003) 197.
[31] H. Kao, Y. Tsai, S. Chao, Solid State Ionics 176 (2005) 1261.
[32] F. Guo, Q. Zhang, B. Zhang, H. Zhang, L. Zhang, Polymer 50 (2009) 1887.